Pterostilbene induces cell apoptosis and inhibits lipogenesis in SKOV3 ovarian cancer cells by activation of AMPK-induced inhibition of Akt/mTOR signaling cascade

Attalla EL-KOTT[1,2]; Eman ELBEALY[3]; Fahmy ELSAID[1,4]; Haitham EL-MEKKAWY[1]; Abd-El-karim ABD-LATEIF[5]; Abdulali TAWEEL[6]; Heba KHALIFA[2]; Ahmad KANDEEL[5]; Kareem MORSY[1,7]; Essam IBRAHIM[1,8,9]; Mashael Mohammed BIN-MEFERIJ[10,*]

[1] Biology Department, College of Science, King Khalid University, Abha, 61413, Saudi Arabia
[2] Zoology Department, College of Science, Damanhour University, Damanhour, 22511, Egypt
[3] Biology Department, College of Science for Girls, King Khalid University, Abha, 61413, Saudi Arabia
[4] Zoology Department, College of Science, Mansoura University, Mansoura, 35511, Egypt
[5] Zoology Department, College of Science, Fayoum University, Fayoum, 63511, Egypt
[6] Zoology Department, Faculty of Science, Al-Zawia University, Al-Zawia, Libya
[7] Biology Department, Faculty of Science, Cairo University, Cairo, 12611, Egypt
[8] Research Center for Advanced Materials Science (RCAMS), King Khalid University, Abha, 61413, Saudi Arabia
[9] Blood Products Quality Control and Research Department, National Organization for Research and Control of Biologicals, Cairo, 12611, Egypt
[10] Biology Department, College of Science, Princess Nourah bint Abdulrahman University, Riyadh, Saudi Arabia

Abstract: This study investigates if the anti-tumor effect of Pterostilbene in the SKOV3 ovarian cancer (OC) cell line involves inhibition of cell metabolism and tested in this effect involves modulating AMPK and Akt-induced regulation of mTORC1. Initially, SKOV3 cells were cultured in the humidified conditions in DMEM media for 24 h with or without increasing concentration of Pterostilbene. Then, the cells were incubated with Pterostilbene (IC_{50} = 50 μM) under similar conditions with or without pre-incubation with Dorsomorphin, an AMPK inhibitor. In a dose-dependent manner, Pterostilbene inhibited SKOV3 cell survival and increased their lysate levels of lactate dehydrogenase (LDH) and single-stranded DNA (ssDNA). When SKOV3 cells were treated with 50 μM Pterostilbene, Pterostilbene significantly suppressed cell migration and invasion, reduced lysate levels of lactic acid and the optical density of Oil Red O staining, and increased lysate glucose levels. It also increased levels of malondialdehyde (MDA), reactive oxygen species (ROS), and induced intrinsic cell apoptosis by upregulating protein levels of Bax and cleaved caspase-3 and reducing protein levels of Bcl-2. Besides, Pterostilbene reduced mRNA levels of sterol regulatory element-binding protein 1 (SREBP-1), fatty acid synthase (FAS), acetyl CoA carboxylase-1 (ACC-1), and AMP-activated protein kinase (AMPK). Furthermore, Pterostilbene increased the protein levels of p-AMPK, p-p53, p-raptor, p-TSC-2, but significantly decreased protein levels of p-Akt, p-TSC-2, p-mTOR, p-S6K1, and p-4E-BP. Treatment with Dorsomorphin (CC) abolished all the anti-tumorigenesis effects afforded by Pterostilbene and prevented Pterostilbene-induced phosphorylation of Akt, p53, and mTOR. In conclusion, the tumor-suppressive effect of Pterostilbene in SKOV3 cells involves the induction of ROS and inhibition of dysregulation cell metabolism mainly due to AMPK-induced Akt-dependent or independent suppression of mTOR.

Introduction

Ovarian cancer (OC) is a common gynecological malignancy that usually affects postmenopausal women (Wang et al., 2005).

Currently, the available treatment of OC involves surgical resection, followed by adjuvant systemic chemotherapy that consists of a combination of platinum and/or taxane-based chemotherapy (Elias et al., 2018). However, the mortality rates remain very high among patients with OC, where the overall 5-year survival rate is less than 40% (Webb and Jordan, 2017). This has been attributed to a lack of symptoms during the initial phases (poor detection),

resistance to chemotherapy, and high recurrence rates (Rooth, 2013; Elias *et al.*, 2018). Despite the extensive clinical trials that have aimed to improve survival and cure rates by early detection, changing the dosing of the chemotherapeutic drugs and the use of combination chemotherapies, these rates didn't significantly change (Bast *et al.*, 2007; Dobbin and Landen, 2013; Elias *et al.*, 2018). This could be explained by the complexity of the disease. Therefore, more understanding of the molecular basis of the disease to identify the major key players in the pathogenesis of the OC and more effective trials to develop more effective drugs that target these pathways is emerging.

Metabolic dysregulation (i.e., higher rates of glucose uptake, protein synthesis, glycolysis, and lipogenesis) is a crucial mechanism for the growth, proliferation, and differentiation of many most solid tumors, including OC (Elstrom *et al.*, 2004; Li *et al.*, 2001; Okawa *et al.*, 2008; Vander Heiden *et al.*, 2009; Wang *et al.*, 2016). Current investigations have identified the mammalian target of rapamycin (mTOR) signaling as an important nutrient sensor pathway in cancer development of most solid tumors, including the OC, by promoting cancer cells metabolism to fulfill their nutrient demands, and it is the major mechanism responsible for the induction of such metabolic dysregulation (Kuhajda, 2008; Lien *et al.*, 2016; Memmott and Dennis, 2009; Mossmann *et al.*, 2018; Su *et al.*, 2019; Tian *et al.*, 2019). Indeed, the activation of mTOR signaling is an essential pathway that enhances cell growth cancer and metastasis cells by increasing ribosomes, protein and purines synthesis, promoting glucose uptake and lipogenesis, and regulating cell cycle by allowing the translation of many pro-oncogenes (Düvel *et al.*, 2010; Ben-Sahra *et al.*, 2016; Majumder *et al.*, 2004; Peterson *et al.*, 2011; Tian *et al.*, 2019).

The regulation of mTOR in most cells, including cancer cells, is a very complicated process that involves mainly the phosphoinositide 3-kinases/protein kinase B (PI3K/Akt) and AMP-activated protein kinase (AMPK). mTOR is normally activated by the PI3K/Akt axis but inhibited by AMPK (LoPiccolo *et al.*, 2008; Sohretoglu *et al.*, 2019; Tian *et al.*, 2019). The activities of PI3K/Akt and mTOR are abnormally regulated in most solid tumors and were associated with cancer growth mediated by metabolic dysregulation where the inhibition of these pathways afforded anti-tumorigenesis and tumor suppressor effects (Okawa *et al.*, 2008; Memmott and Dennis, 2009, Tian *et al.*, 2019). On the contrary, the levels and activation of AMPK, a well-known metabolic sensor, and a tumor suppressor molecule are significantly suppressed in most solid tumors including OC and are associated with tumor growth (Liu *et al.*, 2018; Luo *et al.*, 2010; Rattan *et al.*, 2005; Su *et al.*, 2019). In the majority of these studies, the pharmacological activation of AMPK afforded anti-tumorigenic effects by suppressing tumor proliferation, metastasis, and metabolism by activating p53 and p21 and inhibition of Akt/mTOR axis (Liu *et al.*, 2018; Luo *et al.*, 2010; Rattan *et al.*, 2005; Su *et al.*, 2019).

Pterostilbene (trans-3,5-dimethoxy-4'-hydroxystilbene), an analog polyphenol of resveratrol, is a novel anti-cancer molecule that can inhibit the growth, proliferation, and metastasis of many solid tumors by affecting different signaling pathways (Chang *et al.*, 2018; Chen *et al.*, 2018; Liu *et al.*, 2018; McCormack and McFadden, 2012). The beneficial anti-tumorigenesis properties of Pterostilbene were attributed to its unique molecular structure (dimethyl ether), which makes it more lipophilic with higher rates of oral absorption, membrane permeability, bioavailability, and greater cellular uptake than any other polyphenols, including resveratrol (Kapetanovic *et al.*, 2011; Lin *et al.*, 2009). In melanoma, colorectal, breast, and oral cancer cell lines, the tumor suppressor effect of Pterostilbene was mediated by inhibition of Akt and STAT3, downregulation of Bcl-2, and activation of Bax and cytochrome-c (Chakraborty *et al.*, 2010; Chang *et al.*, 2018; Ferrer *et al.*, 2007; McCormack *et al.*, 2011; Priego *et al.*, 2008). Nonetheless, Pterostilbene suppressed the mantle cell lymphoma by inhibiting PI3K/Akt/mTOR signaling cascade (Yu *et al.*, 2018). In p53 positive and negative human prostate cell lines, Pterostilbene induced cell cycle arrest by decreasing the expression cyclins A and E and upregulation of p53, p21, and p27 mainly through activation of AMPK (Lin *et al.*, 2012). Similarly, Pterostilbene also inhibited lipogenesis in multiple myeloma cells by activation of AMPK-induced downregulation of fatty acid synthesis enzymes, acetyl CoA carboxylase (ACC), and fatty acid synthase (FAS) (Mei *et al.*, 2018). These data suggest that Pterostilbene could regulate cell fate and metabolism by modulating PI3K/Akt and AMPK-dependent regulation of mTOR.

However, the tumor-suppressive effect of Pterostilbene in OC was less investigated. The available evidence has shown that Pterostilbene can inhibit OC proliferation and migration by inducing reactive oxygen species (ROS) and apoptosis and suppression inflammation (Pei *et al.*, 2017; Wen *et al.*, 2018). In some studies involving OC cell lines, the chemoprotective effect of Pterostilbene was shown to be through inhibiting the activation extracellular-signal-regulated kinase (ERK), the nuclear factor kappa light chain enhancer of activated B cells (NF-κB), AKT, and STAT-3 (Pei *et al.*, 2017; Wen *et al.*, 2018). However, it is still largely unknown if Pterostilbene could suppress OC by modulating the AMPK/mTOR axis and cell metabolism.

Therefore, in this study, we tested the hypothesis that treating the SKOV-3 OC cell line with Pterostilbene could induce cell death and suppress cell migration and invasion by suppressing cell metabolism mainly by inhibiting mTOR signaling. Besides, we have examined the involvement of Akt and AMPK in this process.

Materials and Methods

Reagents

Dorsomorphin (Compound C; CC), a selective AMPK inhibitor (Cat. No. ab120843, 99%), was purchased from Abcam, Cambridge, UK. Pterostilbene (Cat. No. P1499, > 97 HPLC) and Dimethyl sulfoxide (DMSO) (Cat. No. 276855, > 99.9%) were bought from Sigma Aldrich (MO, USA). Pterostilbene was prepared in DMSO (100 mM as a stock). All other concentrations of Pterostilbene (10, 25, 50, 100 µM), as well as DMSO, were diluted in the culture media. In all treated cells, DMSO final concentration was 0.1%. All

primers sequences used for real-time PCR were designed and supplied from Integrated DNA Technologies, Inc. (Coralville, IA, USA).

Cell culture and experimental design

The Human chemo-resistant cell line, SKOV3, was used in this study and was bought from the American Type Culture Collection. According to the study of Liu *et al.* (2018), the cells were thawed and cultured (1×10^5/mL) in Dulbecco's Modified Eagle's (DMEM) medium containing FBS (10%), penicillin (100 U/mL), and streptomycin (100 μg/mL) (ThermoFisher Scientific Inc, lL, USA) under humidified conditions (95% air, 5% CO_2, 37°C) for 24 h to reach 85% confluence, which was used in the experimental procedure. Under these conditions, the cells were cultured for 24 h with or without increasing concentrations of Pterostilbene (10, 25, 50, 75, and 100 μM). Cell viability was determined in all treatments and was used to calculate the half inhibitory concentration (IC_{50}) of Pterostilbene using the Dose-Response-Inhibition analysis (GraphPad prism V8, Australia). Based on this IC_{50}, another set of experiments was conducted where the cells (1×10^5/mL) were cultured in the presence or absence of Pterostilbene (at its IC_{50}) with or without 1 h pre-incubation with 10 μM Dorsomorphin. In all experiments, control cells were treated only with 0.1% diluted DMSO, as a vehicle. In our preliminary data, 0.1% DMSO did not affect any of the measured parameters. The concentration of Dorsomorphin used in this study was based on our preliminary data which have shown that such concentration is the minimum concentration to completely block the activation of AMPK. A similar concentration of Dorsomorphin was also used in similar studies in SKOV3 and other cell lines (Vucicevic *et al.*, 2011; Yang *et al.*, 2012; Shi *et al.*, 2018). Each experiment (treatment) was conducted as three trials in triplicates.

Determination of cell viability and other biochemical parameters

Cell viability in all treatments was determined by cell counting kit-8 (CCK-8; Cat. No. CK04-13, Dojindo, Kumamoto, Japan). Intracellular levels of Malondialdehyde (MDA) and ROS were measured with assay kits (Cat. No. ab118970; Abcam, Cambridge, UK, and Cat. No. S0033; Beyotime Institute of Biotechnology, Haimen). Levels of lactate dehydrogenase (LDH) in the media were determined using a colorimetric assay kit (Cat. No. ab102526; Abcam, Cambridge, UK). Levels of ssDNA in the media were measured using an ELISA kit (Cat. No. APT225, Millipore, USA). Glucose levels were measured using a colorimetric kit (ab65333, Abcam, Cambridge, UK). Lactic acid levels in the media were measured by a colorimetric assay kit (Cat. No. L256-10, Dojindo, Munich, Germany). Cell lysate caspase-3 activity was measured using a special kit (Cat. No. ab39410, Abcam, Cambridge, UK). All procedures were done following the manufacturer's instructions.

Oil red O staining

Oil red O staining of cultured cells of all treatments was performed according to the procedure established by Lin *et al.* (2012). Briefly, cells were cultured in DMEM media for 24 h in the presence or absence of Pterostilbene at its IC_{50} (50 μM) with or without 1 h pre-incubation of 10 μM Dorsomorphin. The cells were then washed (2X) with ice-cold phosphate buffer saline (PBS/pH = 7.4) and 50% isopropanol. Cells were double washed with the ice-cold PBS and fixed with 4% formaldehyde for 1 h at 4°C. The Red oil stock solution was prepared in isopropanol (3 mg/mL), and the red oil working solution was prepared as 60% of red oil stock solution in ddH_2O. Then, cells of all treatments were incubated, for 1 h at room temperature with this working solution. After that, the cells were washed with PBS and 70% ethanol. Finally, red oil was dissolved by the addition of 250 μL of isopropanol. The plate was read at 510 nm using a plate reader.

Determination of cell apoptosis and death by flow cytometry

Apoptosis in the cells was measured using a special kit that utilizes Annexin V-Fluorescein isothiocyanate (FITC) (Nanjing KGI Biotech. Co., Ltd., Nanjing, China) as per the manufacturer's instruction. In brief, the cells were cultured in DMEM media for 24 h in the presence or absence of 50 μM Pterostilbene with or without 1 h pre-incubation of 10 μM Dorsomorphin (CC). Then, all groups of cells were incubated at room temperature for 10 min with 500 μL binding buffer, 5 μL propidium iodide, and 5 μL Annexin V-FITC solutions (supplied with the kit). Then, flow cytometry was conducted on a FACSCalibur (BD Biosciences, CA, USA).

Migration and invasion assays

These procedures were done as previously described in more detail in our previous studies and as also described by others (33). In brief, For cell migration analysis, a 24-well Transwell polycarbonate insert (8-μm pores, 6.5 mm diameter) was used (Corning Costar, NY, USA). In brief, the cells (5×10^4/mL) were suspended in the DMEM media containing 1% FBS and added to the top chamber with and treated with either DMSO or Pterostilbene (50 μM) with or without 10 μM Dorsomorphin. The lower chamber contained 600 μL of the proper media supplied with 10% FBS as an attractant. After 24 h, the cells migrated at the lower side of the filter were fixed in methanol (15 min/23°C), stained with 0.2% crystal violet solution (15 min/23°C), and then counted under a light microscope (x10/4 fields). A similar procedure, but with 3 h fasting of cells in serum-free DMEM and using Matrigel-coated Corning 5-mm pore size Transwell polycarbonate, was followed for the invasion assay (Mirandola *et al.*, 2014).

Real-time quantitative PCR (qPCR)

All primer sequences used for real-time PCR were adopted from previous studies (Zhou *et al.*, 2009; Jung *et al.*, 2011) and are shown in Tab. 1. The forward and reverse primers were diluted to a final concentration of 10 μL. An RNeasy Mini Kit (Cat. No. 74104, Qiagen, Victoria, Australia) was used to isolate the total RNA. The ratio of 260/280 (a Nanodrop spectrophotometer) was used as a marker of RNA purity. An iScript cDNA synthesis kit (Cat. No. 4106228; BioRad Montreal, Canada) was used to prepare the first-strand cDNA following the manufacturer's instruction.

TABLE 1

Primer sequences used for real-time PCR

Gene	F: Sequence (5'→3')	R: (5'→3')
SREBP1c	GGAGGGGTAGGGCCAACG	AGGGGTGGAGCTCAACTG
FAS	CGCGTGGCCGGCTACTCCTAC	CGGCTGCCACACGCTCCTCT
ACC-1	TTTGACCTCACTGCCATTCC	GCGACTTCCATACCGCATTAC
AMPK-α1	TGCGTGTACGAAGGAAGAATCC	TGTGACTTCCAGGTCTTGGAGTT
18S	GAGTCAACGGATTTGGTCGT	TTGATTTTGGAGGGATCTCG

The PCR reaction contained the following: 0.77 µL nuclease-free water, 2 µL cDNA, 0.15 µL forward primer, 0.15 µL reverse primers, and 10 µL of Ssofast Evergreen Supermix (Cat. NO. 172-5200, BioRad, Montreal, Canada). All PCR runs were conducted in a CFX96 real-time PCR system (Bio-Rad, CA, USA). The qPCR conditions were enzyme inactivation (95°C/30 s/1 cycle), denaturation (95°C/5 s/35 cycles), annealing/extension at (60°C/30 s/35 cycles), and melting (95°C/1 s/1 cycle). The relative expression was calculated using the comparative cycle threshold (Ct) method ($2^{-\Delta\Delta Ct}$). cDNA template was omitted in some wells as control.

Western blotting analysis
Cell pellets were homogenized in an appropriate volume of RIPA lysis buffer plus protease inhibitor cocktail. Protein concentrations were measured by a Pierce BCA assay (Cat. No. 23225, ThermoFisher Scientific). Proteins (40 µg/sample) were separated on different ratios of SDS–polyacrylamide gel and then transferred onto nitrocellulose membranes. Membranes were then blocked with skimmed milk, washed with TBST buffer, and then incubated with primary antibodies (room temperature/2 h/with shaking) against AMPK-α1 (Cat. No. 2532), p-AMPK-α1 (Thr^{172}, Cat No. 2535), FAS (Cat. No. 3180), Akt (Cat. No. 9272), p-Akt (T308, Cat. No. 9275), ribosomal protein S6 kinase beta-1 (S6K1) (Cat. No 9202), mTOR (Cat. No. 2972), p-mTOR (Ser^{2448}) (Cat. No. 2448), p-S6K1 (T389, Cat. No 9205), p-eukaryotic translation initiation factor 4E (eIF4E)-binding protein 1 (p-4E-BP-1) p-4E-BP1 (Thr$^{37/46}$, Cat. NO.2855), p-tuberous sclerosis complex 2 (p-TSC-2) (Thr^{1462}, Cat. No. 3661); p-TCS-2 (Ser^{1387}, Cat. No. 5584, p-regulatory-associated protein of mTOR (p-raptor) (Ser^{792}) (Cat. No. 2083), Bcl-2 (Cat. No. 2876), Bax (Cat. No. 2772, 1:1000), cleaved caspase-3 (Cat. No. 966, 1:1000) (Cell Signalling Technology; USA) and against β-actin (Cat. No. sc-47778, Santa Cruz Biotechnology). Membranes were then washed with Tris-buffered saline-Tween20 (TBST) buffer (3X/each of 10 min) and incubated with the horseradish peroxidase (HRP)–conjugated secondary antibody. All antibodies were always prepared in the TBST buffer. Bands were developed using Pierce ECL reagents (ThermoFisher, USA, Piscataway, NJ) and scanned and analyzed using a C-Di Git blot scanner (LI-COR, NE, USA) and analyzed using the associated software. A single membrane was stripped up to 4 times where the phosphorylated protein forms were detected first, and the reference protein blotted lastly.

Statistical analysis
All data were analyzed using one-way ANOVA, followed by Tukey's test (Graph Pad Prism, V8/Australia). Data were presented as mean ± standard deviation (SD) and considered significantly varied when $p < 0.05$ (Tab. 1).

Results

Pterostilbene inhibited cell survival of SKOV3 cells and increased their release of LDH and ssDNA in a dose-response manner
As shown in Figs. 1A–1C, Pterostilbene, a decrease in the rate of cell survival but significantly increased the medium levels of LDH and ssDNA in SKOV3 cells, in a dose-dependent manner, as compared to control cells. The maximum effect of Pterostilbene on all these parameters was achieved at a concentration of 100 µM, which was not varied with the other higher doses (150 µM and 200 µM). The calculated IC$_{50}$ was determined to be 50 µM and was used for the rest of the experiments.

The pro-oxidant and apoptotic effects of Pterostilbene are AMPK dependent
When tested at its IC$_{50}$ (50 µM), Pterostilbene induced cell apoptosis (as detected by flow cytometry) (Figs. 2AI-III) and increased intracellular levels of ROS, lipid peroxides (MDA), and caspase-3 activity (Figs. 2B–2D) in SKOV3 cells as compared to control cells. It also increased protein levels of Bax and cleaved caspase-3 and concomitantly inhibited protein levels of Bcl-2 in the treated cells as compared to control cells (Fig. 2E). However, cell apoptosis and levels of all these biochemical endpoints were not significantly different when control cells were compared to control + Pterostilbene + Dorsomorphin, the inhibitor of AMPK (Figs. 2A–2E). These data suggested that the pro-oxidant and apoptotic effects of Pterostilbene is AMPK-dependent.

Pterostilbene inhibited cell invasion and migration, glucose uptake, lactate production, and lipid accumulation in SKOV3 cells in an AMPK-dependent manner
As compared to control cells, treating the SKOV3 cells with Pterostilbene at a concentration of 50 µM (IC$_{50}$) significantly lowered the number of migrating and invading cells (Figs. 3A and 3B). Also, Pterostilbene-treated cells had higher levels of glucose and lower levels of lactate in their media with a significant reduction in the optical density of
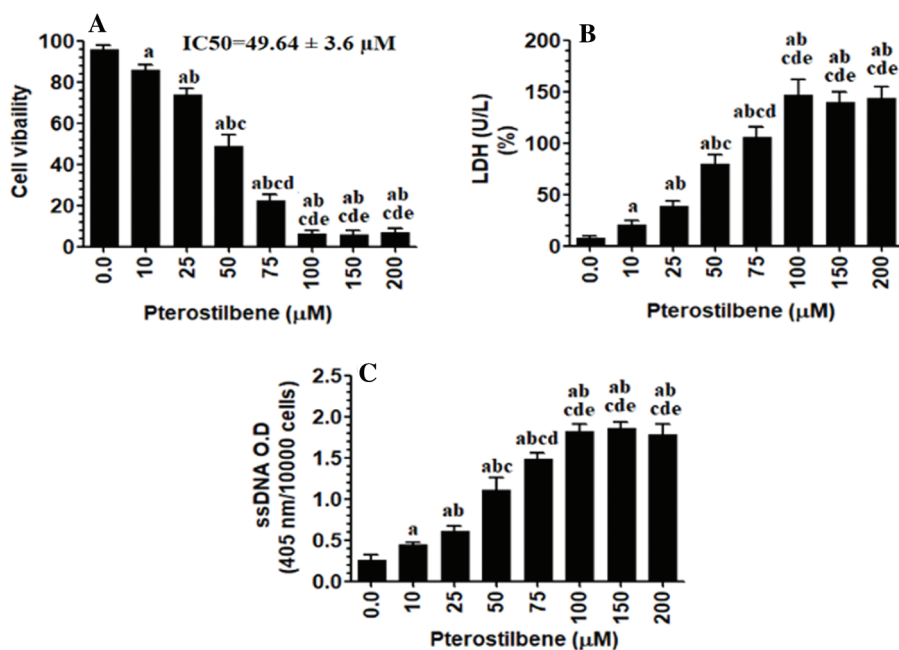
FIGURE 1. Pterostilbene inhibited cell survival of SKOV3 cells and increased their release of LDH and ssDNA, in a dose-response manner.
(A) Cell survival, (B) lactate dehydrogenase (LDH), and (C) single-stranded DNA (ssDNA). Cells were cultured in DMEM media for 24 h in the presence or absence of Pterostilbene. IC50 is identified as the inhibitory concentration that causes a 50% decrease in cell survival. Control cells were treated only with 0.1% DMSO. Data were presented as mean ± SD of three trials each performed in triplicate. Values were considered significantly different at $p < 0.05$. a: $vs.$ Control cells. b: $vs.$ Pterostilbene (10 μM). c: $vs.$ Pterostilbene (25 μM) d: $vs.$ Pterostilbene (50 μM) e: $vs.$ Pterostilbene (75 μM).

oil red O staining as compared to control cells (Figs. 3C–3E). All these effects were completely reversed in Pterostilbene-treated cells which were pre-incubated with Dorsomorphin, and their levels were not significantly different when compared to control cells (Figs. 3A–3E).

Pterostilbene inhibits lipogenesis in SKOV3 cells in an AMPK-dependent manner

mRNA of SREBP-1, FAS, ACC-1, and AMPK, as well as protein levels of FAS and ACC-1, were significantly reduced in Pterostilbene-treated cells (at IC_{50} = 50 μM) as compared to control cells (Figs. 4A–4F). The levels of these markers were not significantly different between control and Pterostilbene + Dorsomorphin (CC) treated cells (Figs. 4A–4F). These data suggest that Pterostilbene suppresses the transcription factor SREBP-1 and its downstream fatty acid synthesis genes through an AMPK-dependent mechanism.

Pterostilbene activated AMPK but inhibited the activity of Akt, mTORC1, and p53

mTOR activation induces phosphorylation of S6K1 and 4E-BP1, which mediate all its cellular events (Tian *et al.,* 2019). However, TSC-2 and raptor are a cellular inhibitor of mTOR (Tian *et al.,* 2019). PI3K/Akt activates mTOR by phosphorylation at p-TSC-2 (Thr[1462]), which results in inhibition of TSC-2 (LoPiccolo *et al.,* 2008; Tian *et al.,* 2019). On the contrary, AMPK inhibits mTOR by activation of TSC-2 through phosphorylating it at Ser[1387]. Also, AMPK inhibits mTOR by phosphorylation and activation of raptor at Ser[792] (Sohretoglu *et al.,* 2019). As shown in Figs. 5A–5C, with stable total protein levels of AMPK, Akt, and p53, treating the SKOV3 cells with Pterostilbene at an IC_{50} of 50 μM significantly increased protein levels of p-AMPK (Thr[172]) and p-p53 (Ser[15]) but significantly decreased protein levels of p-Akt (Thr[308]) as compared to control cells. Also, Pterostilbene increased the phosphorylation of the two downstream targets of AMPK, named p-TSC-2 (Ser[1387]) and raptor (Ser[792]) (Figs. 5D and 6D), which normally inhibit

mTORC1 when they are Pterostilbene also reduced protein levels of p-TSC-2 (Thr[1462]), a major target of Akt (activation) (Fig. 5D) These data suggest that Pterostilbene can inhibit mTORC1 signaling by activation of TSC-2 through either activating AMPK or suppressing Akt. To confirm this, we have measured levels of mTOR/p-mTOR (Ser[2448]) and the phosphorylation rate of its downstream targets S6K71 and p-4E-BP1. Supporting our hypothesis, and with no change in total levels of mTOR, Pterostilbene-treated cells showed lower protein levels of p-mTOR (Ser[2448]), pS6K71 (Thr[389]), and p-4E-BP1 (Thr[37/46]) (Figs. 6A and 6C, respectively). However, the effects of Pterostilbene on all these biochemical parameters in the treated cells were prevented by Dorsomorphin (Figs. 5A–5D and 6A–6D). These data suggest that Pterostilbene activates p53 and inhibits Akt and mTOR through activation of AMPK.

Discussion

The findings of this study support the anti-tumorigenic effect of Pterostilbene in the SKOV3 OC cell line is associated with suppressing the dysregulated cell metabolism. In particular, treating the SKOV3 cells with Pterostilbene not only suppressed glucose uptake and the production of lactic acid but also reduced intracellular lipid accumulation, stimulated cell apoptosis, and suppressed cell migration and invasion. These effects were associated with a reduction in the activity of Akt/mTOR signaling and concomitant activation of AMPK and p53. Of note, pretreating the cells with Dorsomorphin, an AMPK inhibitor, completely prevented all the effects afforded by Pterostilbene, thus suggesting that the anti-tumorigenic effect of Pterostilbene is an AMPK-dependent.

The intrinsic cell apoptosis is a very regulated mechanism that depends largely on a delicate balance between apoptotic (i.e., Bax) and anti-apoptotic (i.e., Bcl2) (Redza-Dutordoir and Averill-Bates, 2016). ROS and subsequent induction of DNA damage and activation of p53
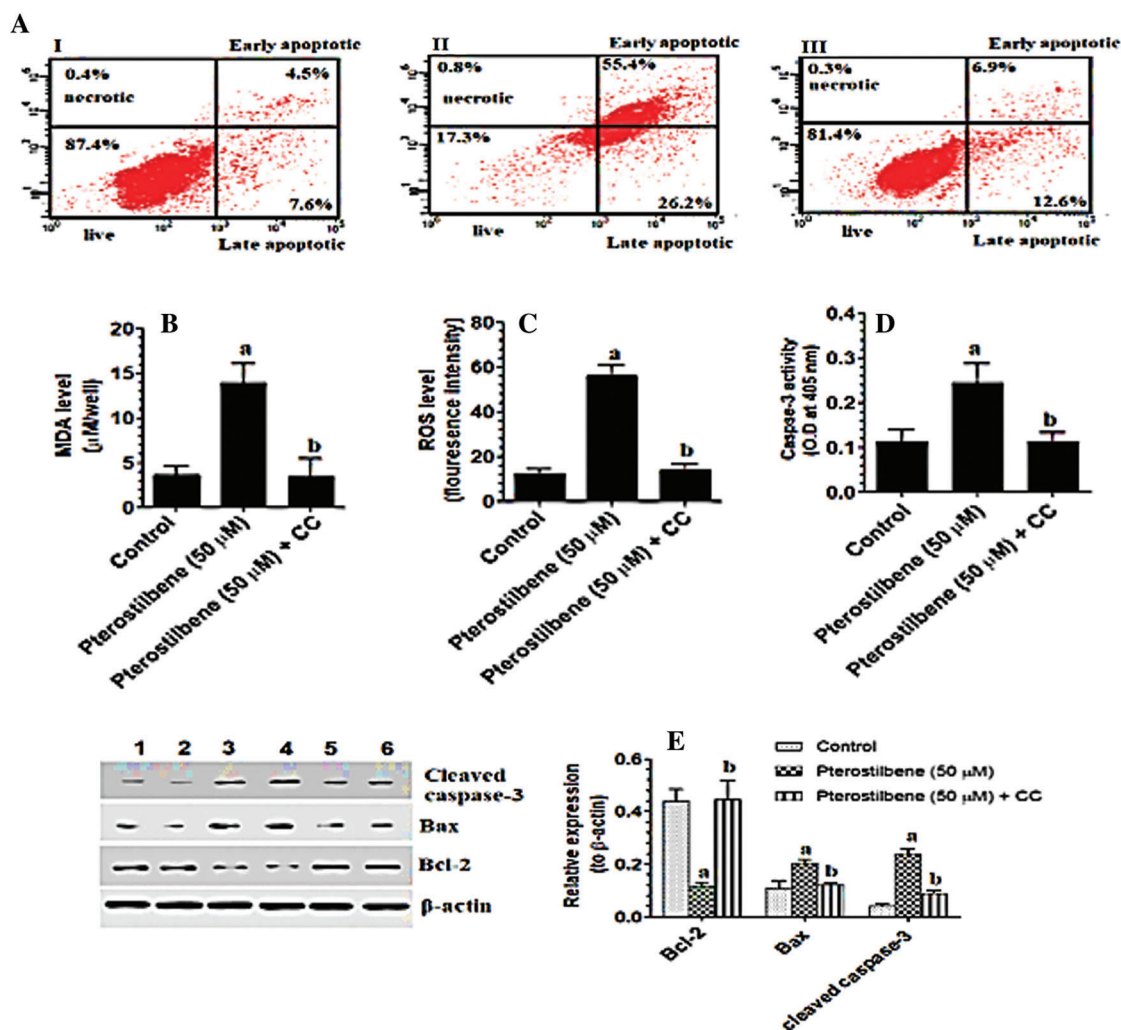
FIGURE 2. Pterostilbene stimulated cell apoptosis and necrosis, increased the levels of malondialdehyde (MDA) and reactive oxygen species (ROS), and the activity of caspase-3, upregulated protein levels of cleaved caspase-3 and Bax, and downregulated protein levels of BCl-2 in SKOV3 cells, in an AMPK-dependent manner.

(A) Cell apoptosis and necrosis as detected by flow cytometry, (B) lysate levels of MDA, (C) lysate levels of ROS, (D) lysate activity of caspase-3, and (E) protein levels of cleaved caspase-3, Bax, and Bcl-2. Cells were cultured in DMEM media for 24 h in the presence or absence of Pterostilbene at its IC50 (50 μM) with or without 1 h pre-incubation of 10 μM Dorsomorphin (compound C; CC), an AMPK inhibitor. Control cells were treated with 0.1% DMSO. In panel A; I: control cells, II: Pterostilbene-treated cells, III: Pterostilbene + CC-treated cells. In panels B-E: Data were presented as mean ± SD of three trials each performed in triplicate. Values were considered significantly different at $p < 0.05$. a: *vs.* Control cells. b: *vs.* Pterostilbene-treated cells. In panel E: Lanes 1 and 2: Control cells; Lanes 3 and 4: Pterostilbene-treated cells; and Lanes 5 and 6: Cells co-treated with Pterostilbene + CC.

are well-believed to be the major mechanisms that activate intrinsic cell death (Redza-Dutordoir and Averill-Bates, 2016). Accordingly, it is well accepted that p53 stimulates the mitochondria-mediated cell apoptosis by activating Bax and reducing the Bcl-2/Bax ratio (Chipuk *et al.,* 2004). Currently, it is well accepted that inactivation of the p53 pathway and apoptosis is a fundamental event in the pathogenies of most human cancers (Aylon and Oren, 2011; Jackson and Lozano, 2013). In this study, we have shown that Pterostilbene was very effective in inducing intrinsic cell death and suppressing cell migration and invasion in the SKOV3 cells by inducing ROS, activation of p53, upregulating Bax, and suppressing Bcl-2. These data are not strange given the long apoptotic history of Pterostilbene in various cell lines, including breast cancer, gastric cancer, OC, oral cancer, leukemia, lung cancer (Wang and Chen, 2014). Supporting our data, Pterostilbene activated intrinsic

cell death by increasing ROS generation and Ca^{2+} overload (Pan *et al.,* 2009; Wang *et al.,* 2010).

Although p53 is directly activated by ROS, it has been also shown that p53 is a target of AMPK (Rattan *et al.,* 2005). Indeed, in multiple cancer cells, AICAR, an AMPK activator, inhibited the proliferation of various cells by increasing the expression of p21 and p53 (Rattan *et al.,* 2005). Also, AMPK can directly activate p53 through inhibiting NDM2, a natural inhibitor of p53 (Jones *et al.,* 2005). Also, AMPK is an important apoptotic induces that can induce cell death by stimulating the generation of ROS from the mitochondria by suppressing the electron transport chain, activating JNK, P53, and caspase-3, and inhibition of mTORC1 and Bcl-2 (Villanueva-Paz *et al.,* 2016). However, p53 can also upregulate and activate AMAPK (Feng *et al.,* 2007). In this study and associated with the oxidative stress and apoptotic responses, as well as the increased activation
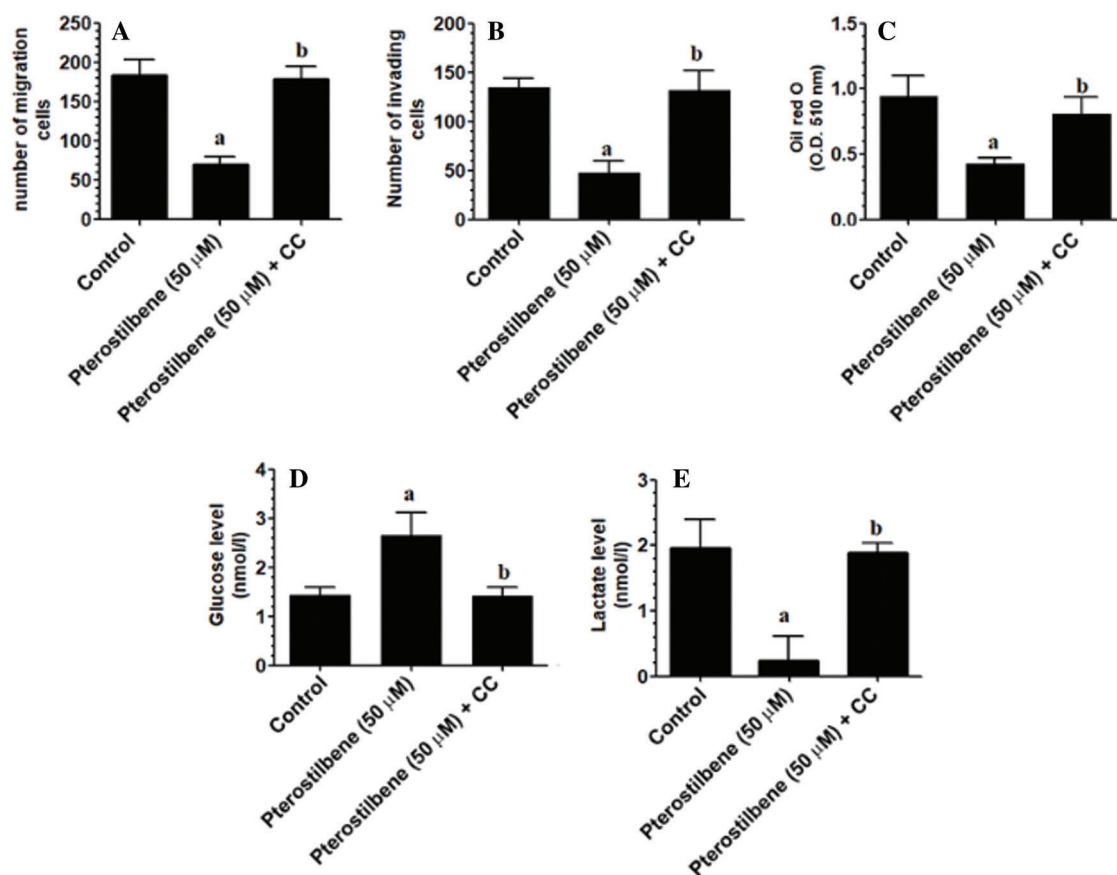
FIGURE 3. Pterostilbene inhibited cell invasion and migration, glucose uptake, lactate production, and lipid accumulation in SKOV3 cells in an AMPK-dependent manner.

(A) Rate of cell migration, (B) Rate of cell invasion, (C) Homogeneous absorbance of oil red O staining, (D) Lysate levels of glucose, and (E) Lysate levels of lactic acid (lactate). Cells were cultured in DMEM media for 24 h in the presence or absence of Pterostilbene at its IC50 (50 μM) with or without 1 h pre-incubation of 10 μM Dorsomorphin (compound C; CC), an AMPK inhibitor. Control cells were treated with 0.1% DMSO. Data were presented as mean ± SD of three trials, each performed in triplicate. Values were considered significantly different at $p < 0.05$. a: *vs.* Control cells. b: *vs.* Pterostilbene-treated cells.

of p53, Pterostilbene also increased the activation of AMPK. Of interest, Dorsomorphin completely prevented Pterostilbene-induced cell apoptosis, the increase in the levels of ROS, and the activation of p53 and stimulated cell survival. Based on these data, we became very confident that the anti-tumorigenesis of Pterostilbene is an AMPK-dependent process. It also indicates that the pro-oxidant and apoptotic effect of Pterostilbene, as well as the Pterostilbene-induced activation of p53, is AMPK-dependent, thus mimicking the above-mentioned effect exerted by AICAR (Rattan *et al.,* 2005). Supporting these data, Pterostilbene inhibited p53 in human prostate cell lines proliferation by activation of AMPK (Lin *et al.,* 2012).

Nonetheless, the metabolism of most cancer cells is reprogrammed toward high glucose uptake, glycolysis, and lipid synthesis to facilitate cell growth, proliferation, and invasiveness (Vander Heiden *et al.,* 2009). Increased anaerobic glycolysis, lactic acid production, and abnormally overexpressed FAS and ACC-1 were shown in most cancer cells (Thupari *et al.,* 2001; Vander Heiden *et al.,* 2009; Wang *et al.,* 2016; Zadra *et al.,* 2019). Within this view, the newly synthesized lipids present an important integral part of the new cell and organelle membranes and can affect membrane biogenesis, signal transduction, and intracellular trafficking, and modify lipid-based to enhance cancer cell

survival (Baron *et al.,* 2004; Santos and Schulze, 2012). Also, it was shown that lactate levels create an acidic environment that is required for the activation of metalloproteinases (MMPs), which in turn stimulates cancer cell migration and invasion (Cairns *et al.,* 2011; Gentric *et al.,* 2017). mTOR signaling pathway (mTOR/S6K1/4E-BP1) is the major nutrient, metabolic, and sensor pathway to fulfilling their nutrient demands (Tian *et al.,* 2019). In this view, mTORC1 singling promotes cell cycle progression cell growth by promoting protein synthesis through increasing ribosome biosynthesis and the translation of specific pro-oncogenes (Tian *et al.,* 2019). Also, mTOR signaling increases the expression of a variety of glycolytic enzymes through stimulating the expression and translation of hypoxia-inducible factor-1α and Myc and activation of Akt (Düvel *et al.,* 2010; Elstrom *et al.,* 2004; Majumder *et al.,* 2004). Besides, mOTRC1 stimulates lipogenesis by inducing the transcription and translation of SREBP-1 and their downstream fatty acid and cholesterol synthesis genes, including ACC-1 and FAS (Peterson *et al.,* 2011; Porstmann *et al.,* 2008). Furthermore, mTOR stimulates the synthesis of purine and pyrimidine needed for DNA synthesis of the cancer cells (Ben-Sahra *et al.,* 2016).

In this study and associated with the reduction in cell survival and migration/invasion rate, Pterostilbene also
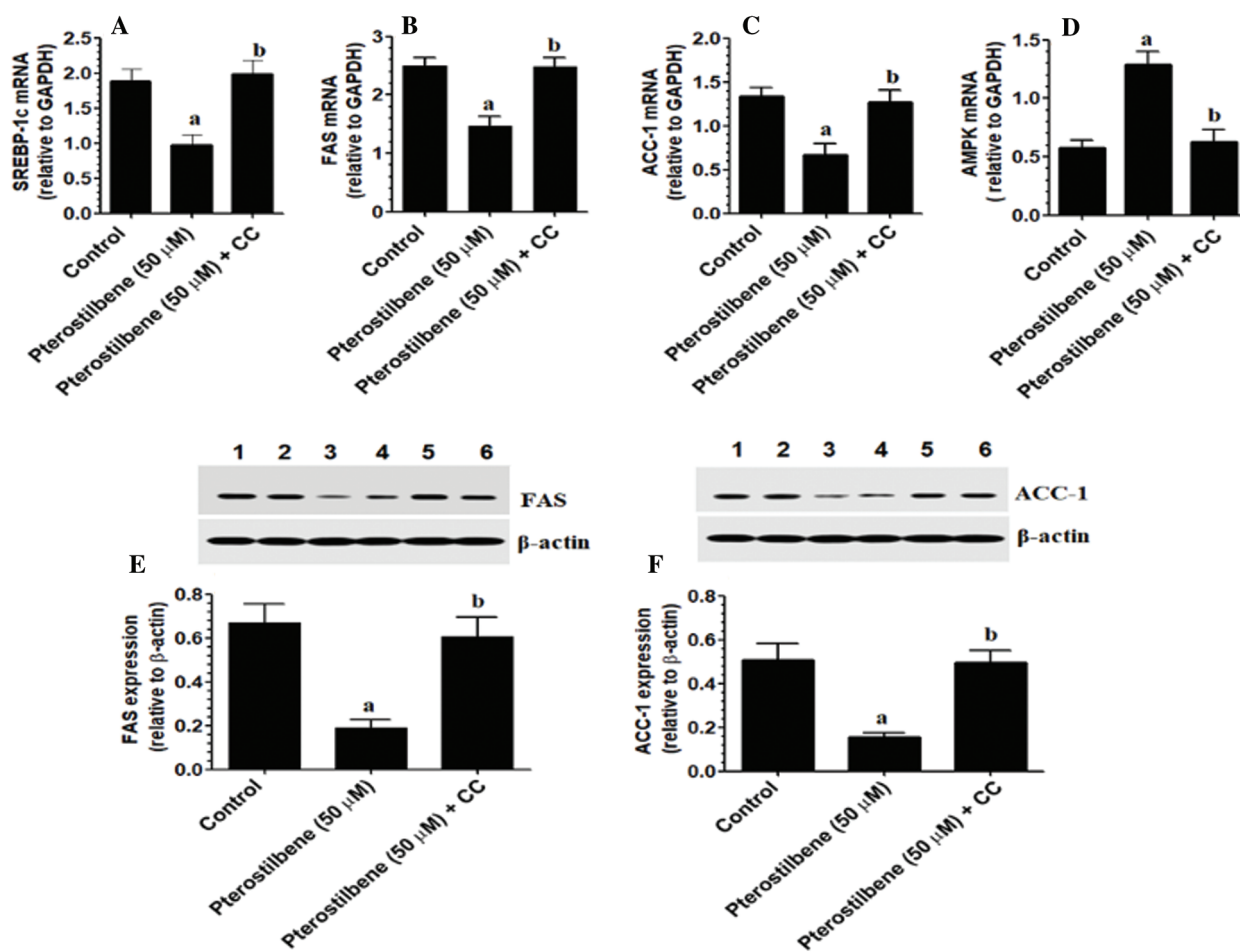
FIGURE 4. Pterostilbene inhibited the transcription of AMPK and suppressed lipogenesis by downregulating the mRNA expression of SREBP-1 and mRNA and protein levels of major lipid synthesis genes in SKOV3 cells in an AMPK-dependent manner.

(A) mRNA levels of SREBP-1, (B) mRNA levels of fatty acid synthase (FAS), (C) mRNA levels of acyl Co-carboxylase-1 (ACC-1), (D) mRNA levels of AMPK, (E) protein levels of FAs, and (F) protein levels of ACC-1. Cells were cultured in DMEM media for 24 h in the presence or absence of 50 μM Pterostilbene, with or without 1 h pre-incubation of 10 μM Dorsomorphin (compound C; CC), an AMPK inhibitor. Control cells were treated with 0.1% DMSO. Data were presented as mean ± SD of three trials, each performed in triplicate. Values were considered significantly different at $p < 0.05$. a: *vs.* Control cells. b: *vs.* Pterostilbene-treated cells. In panels E-F: Lanes 1 and 2: Control untreated cells; Lanes 3 and 4: Pterostilbene-treated cells, and Lanes 5 and 6: Cells co-treated with Pterostilbene + CC.

inhibited mTORC1 signaling in the cultured SKOV-3 cells, as evidenced by the significant decrease in the phosphorylation of mTOR and its downstream targets, p-S6K1 and p- 4E-BP1. Associated with these changes, Pterostilbene-treated cells had higher levels of glucose and reduced levels of lactic acid, the lower optical density of oil red O stain (lipids), and reduced mRNA levels of SREBP1, FAS, and ACC-1 and protein levels of FAS and ACC-1. These data suggest that the inhibitory effect of Pterostilbene on cell survival, migration, and invasion is mediated by altering the dysregulated cancer metabolism, mainly through suppressing glucose uptake and lipogenesis through suppressing of mTORC1 signaling. However, the mechanism by which Pterostilbene induces such regulation on mTOR became very challenging to us and our next target.

In general, the activation of mTOR is a very complicated process that involves numerous signaling pathways. On the one hand, Akt could activate mTORC1 by phosphorylation (inactivation) of the TSC-2 (at Ser[939] and Thr[1462]), which normally inhibits mTOR through the GTP-binding protein Ras homolog enriched in brain (Rheb) (LoPiccolo et al., 2008;

Tian et al., 2019). On the other hand, and independent of Akt, AMPK can inhibit mTORC1 by phosphorylation and activation of TCS-2 by direct phosphorylation of multiple sites, including Ser[1387] (Sohretoglu et al., 2019). Also, AMPK induces the phosphorylation of raptor at Ser[792], which in turn phosphorylates and inhibits the mTORC1 complex (Sohretoglu et al., 2019). In this study and associated with the reduced phosphorylation of Akt (inhibition), Pterostilbene significantly reduced phosphorylation of p-TSC-2 (Thr[1462]), which indicates an over-activated TSC-2. Besides, and associated with increased activity of AMPK, Pterostilbene also induced phosphorylation (activation) of p-TCS-2 at Ser[1387], a major AMPK downstream target, and stimulated the phosphorylation of raptor. These data suggest that Pterostilbene-induced inhibition of mTOR involves suppression of Akt and activation of the AMPK/TCS/raptor pathway.

AICAR, an AMPK activator also PI3K/Akt signaling pathway some cancer types, thus suggesting an upstream regulation of AMPK on Akt (Rattan et al., 2005). An
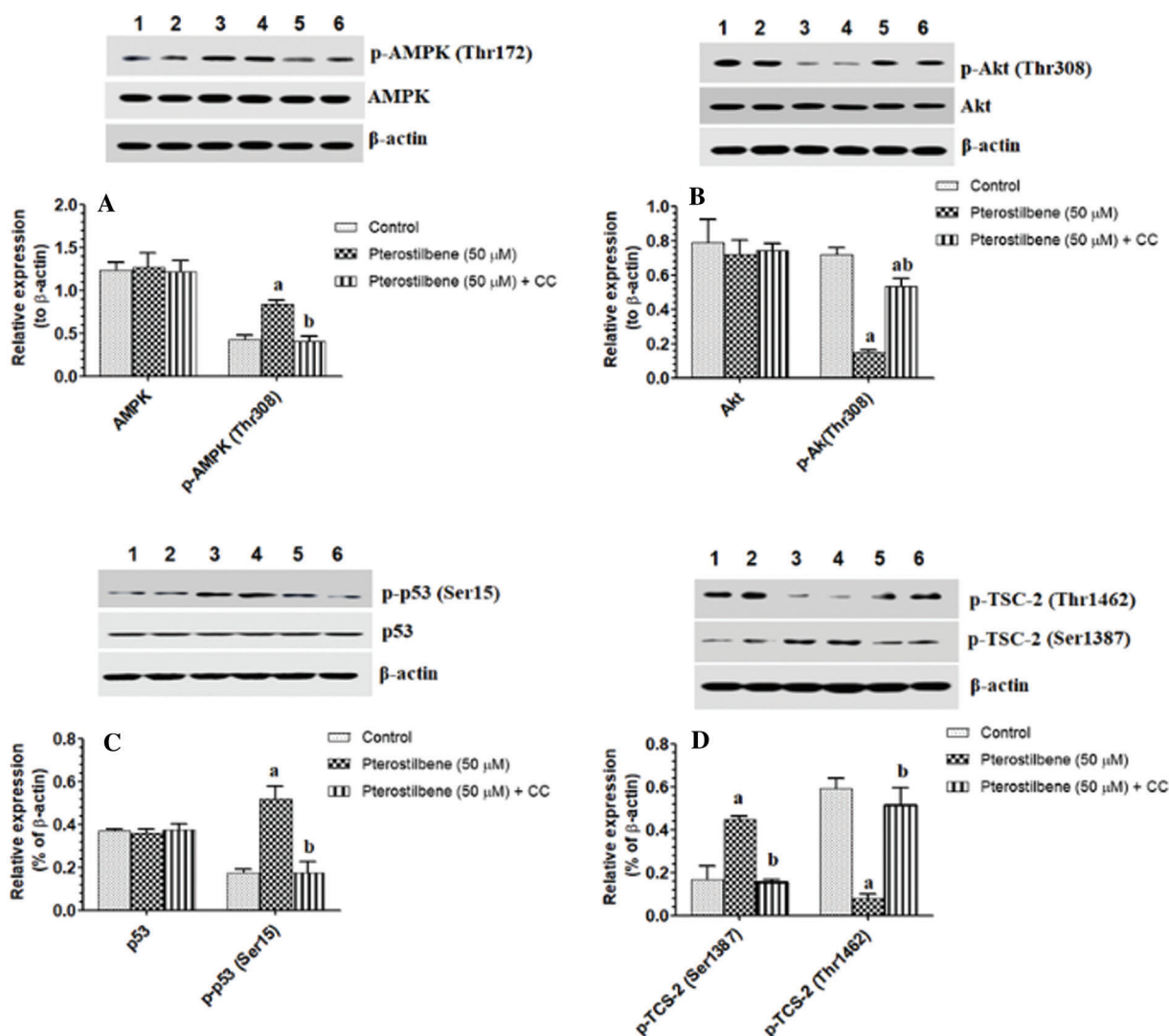
FIGURE 5. Pterostilbene activated AMPK/P53 axis and modulated the activity of TSC-2 in the SKOV-3 cells.
(A) Protein levels of total AMPK/phospho-AMPK, (B) Protein levels of total Akt/phospho-Akt (Thr308), (C) Protein levels of total p53/phospho-p53, and (D) Protein levels of phospho-TSC-2 (Thr1462 and Ser1387). Cells were cultured in DMEM media for 24 h in the presence or absence of Pterostilbene at its IC50 (50 μM) with or without 1 h pre-incubation of 10 μM Dorsomorphin (compound C; CC), an AMPK inhibitor. Control cells were treated with 0.1% DMSO. Data were presented as mean ± SD of three trials, each performed in triplicate. Values were considered significantly different at $p < 0.05$ a: $vs.$ Control cells. b: $vs.$ Pterostilbene-treated cells. In panels A-D: Lanes 1 and 2: Control cells; Lanes 3 and 4: Pterostilbene-treated cells, and Lanes 5 and 6: Cells co-treated with Pterostilbene + CC.

interesting observation in this study Dorsomorphin also suppressed the phosphorylation Akt. Besides, Dorsomorphin prevented the activation of mTOR signaling and prevented Pterostilbene-induced downregulation of SREBP-1c, FAS, and ACC-1, and suppression of glucose uptake and lactate production. Therefore, it seems very reasonable that the inhibitory effect of Pterostilbene on lipogenesis and Akt and mTOR activation is an AMPK-dependent, and activation of AMPK is the major mechanism that mediates all the anti-tumorigenesis role of Pterostilbene. In support, Lin et al. (2012) showed that Pterostilbene can suppress lipogenesis in p53 prostate cancer cells through activation of AMPK-induced inhibition of mTOR in an Akt-dependent or independent manner (Lin et al., 2012). Also, Resveratrol, an analog of Pterostilbene, inhibited the proliferation of SKOV3 and A2780 OC cell lines through inhibiting glycolysis and AMPK/mTOR axis (Liu et al., 2018).

Despite these interesting data, our manuscript still has some limitations. Importantly, this study still investigating the effect of Pterostilbene only SKOV3 cell lines. To confirm this effect, this effect should be examined in more OC cell lines, as well as in vivo. Also, this study lacks a positive control (AMPK activator) such as resveratrol and Ampkinone (Calbiochem) to compare our results. Besides, it has been suggested that energy depletion, such as that which happens with metformin, is the major mechanism for the induction of AMPK (Rena et al., 2017; Yan et al., 2018). Besides, several intracellular pathways can regulate AMPK activity (Yan et al., 2018). In this study, the precise mechanism by which Pterostilbene induced activation of AMPK was not investigated. Therefore, future studies should consider this.

In conclusion, this study is the first to show that the Pterostilbene tumor suppression effect in SKOV3 cell lines
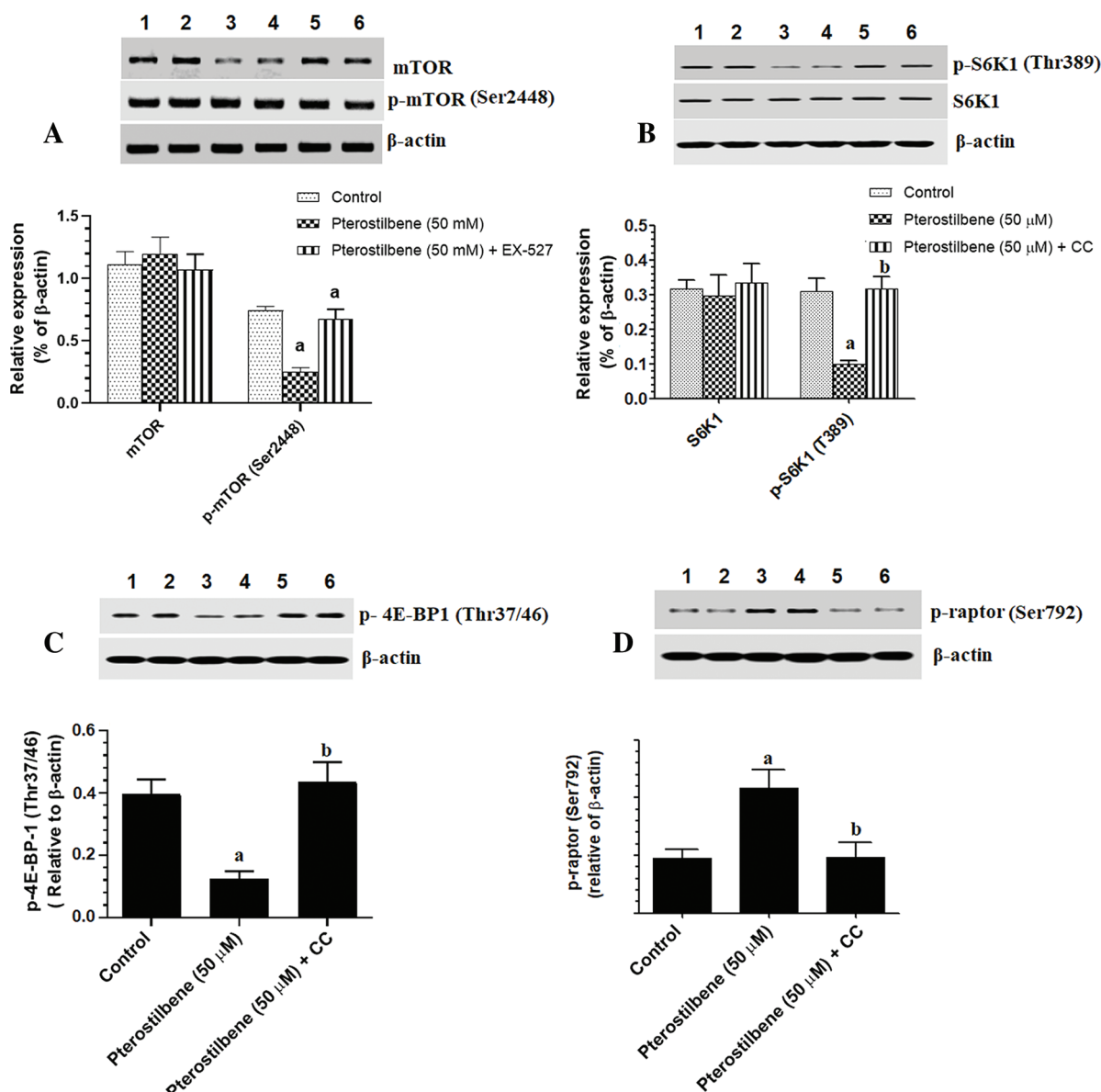
FIGURE 6. Protein levels of mTOR/p-mTOR (A), 6SK1/pS6K1 (B), p-4EBP1 (C), and p-raptor (D) in the SKOV-3 cell homogenates of all treatments.

Cells were cultured in DMEM media for 24 h in the presence or absence of Pterostilbene at its IC50 (50 µM) with or without 1 h pre-incubation of 10 µM compound C (CC), an AMPK inhibitor. Data were presented as mean ± SD of three trials each performed in triplicate. Values were considered significantly different at $p < 0.05$. a: *vs.* Control untreated cells (lanes 1 & 2). b: *vs.* Pterostilbene (lanes 3 & 4). Lanes 5 & 6 were taken from cells co-treated with Pterostilbene + CC.

involves inhibition of apoptosis, glucose uptake, and lipogenesis. It also demonstrates the possible mechanism of action that is mediated, at least, by activation of AMPK and subsequent inhibition of Akt dependent or independent mTORC1 activity.

Availability of Data and Materials: The data used to support the findings of this study are available from the corresponding author upon request.

Ethical approval: All applicable international, national, and/or institutional guidelines for the care and use of animals and cell lines were followed and approved by the ethical committee at the Princess Nourah bint Abdulrahman University, Riyadh, Saudi Arabia.

Conflicts of Interest: The authors have declared no conflict of interest.

References

Aylon Y, Oren M (2011). New plays in the p53 theater. *Current Opinion in Genetics & Development* **21**: 86–92. DOI 10.1016/j.gde.2010.10.002.

Bast RC, Brewer M, Zou C, Hernandez MA, Daley M, Ozols R, Lu K, Lu Z, Badgwell D, Mills GB (2007). Prevention and early

detection of ovarian cancer: mission impossible?, *Cancer Prevention Springer*. Berlin, Heidelberg: Springer, 91–100.

Baron A, Migita T, Tang D, Loda M (2004). Fatty acid synthase: A metabolic oncogene in prostate cancer? *Journal of Cellular Biochemistry* **91**: 47–53. DOI 10.1002/jcb.10708.

Ben-Sahra I, Hoxhaj G, Ricoult SJ, Asara JM, Manning BD (2016). mTORC1 induces purine synthesis through control of the mitochondrial tetrahydrofolate cycle. *Science* **351**: 728–733. DOI 10.1126/science.aad0489.

Cairns RA, Harris IS, Mak TW (2011). Regulation of cancer cell metabolism. *Nature Reviews Cancer* **11**: 85–95. DOI 10.1038/nrc2981.

Chakraborty A, Gupta N, Ghosh K, Roy P (2010). *In vitro* evaluation of the cytotoxic, anti-proliferative and anti-oxidant properties of pterostilbene isolated from *Pterocarpus marsupium*. *Toxicology in Vitro* **24**: 1215–1228. DOI 10.1016/j.tiv.2010.02.007.

Chang HP, Lu CC, Chiang JH, Tsai FJ, Juan YN, Tsao JW, Chiu HY, Yang JS (2018). Pterostilbene modulates the suppression of multidrug resistance protein 1 and triggers autophagic and apoptotic mechanisms in cisplatin-resistant human oral cancer CAR cells via AKT signaling. *International Journal of Oncology* **52**: 1504–1514.

Chen RJ, Kuo HC, Cheng LH, Lee YH, Chang WT, Wang B Jr, Wang YJ, Cheng HC (2018). Apoptotic and nonapoptotic activities of pterostilbene against cancer. *International Journal of Molecular Sciences* **19**: 287. DOI 10.3390/ijms19010287.

Chipuk JE, Kuwana T, Bouchier-Hayes L, Droin NM, Newmeyer DD, Schuler M, Green DR (2004). Direct activation of Bax by p53 mediates mitochondrial membrane permeabilization and apoptosis. *Science* **303**: 1010–1014. DOI 10.1126/science.1092734.

Dobbin ZC, Landen CN (2013). The importance of the PI3K/AKT/MTOR pathway in the progression of ovarian cancer. *International Journal of Molecular Sciences* **14**: 8213–8227. DOI 10.3390/ijms14048213.

Düvel K, Yecies JL, Menon S, Raman P, Lipovsky AI, Souza AL, Triantafellow E, Ma Q, Gorski R, Cleaver S (2010). Activation of a metabolic gene regulatory network downstream of mTOR complex 1. *Molecular Cell* **39**: 171–183. DOI 10.1016/j.molcel.2010.06.022.

Elias KM, Guo J, Bast RC (2018). Early detection of ovarian cancer. *Hematology/Oncology Clinics of North America* **32**: 903–914. DOI 10.1016/j.hoc.2018.07.003.

Elstrom RL, Bauer DE, Buzzai M, Karnauskas R, Harris MH, Plas DR, Zhuang H, Cinalli RM, Alavi A, Rudin CM (2004). Akt stimulates aerobic glycolysis in cancer cells. *Cancer Research* **64**: 3892–3899. DOI 10.1158/0008-5472.CAN-03-2904.

Feng Z, Hu W, De Stanchina E, Teresky AK, Jin S, Lowe S, Levine AJ (2007). The regulation of AMPK β1, TSC2, and PTEN expression by p53: stress, cell and tissue specificity, and the role of these gene products in modulating the IGF-1-AKT-mTOR pathways. *Cancer Research* **67**: 3043–3053. DOI 10.1158/0008-5472.CAN-06-4149.

Ferrer P, Asensi M, Priego S, Benlloch M, Mena S, Ortega A, Obrador E, Esteve JM, Estrela JM (2007). Nitric oxide mediates natural polyphenol-induced Bcl-2 down-regulation and activation of cell death in metastatic B16 melanoma. *Journal of Biological Chemistry* **282**: 2880–2890. DOI 10.1074/jbc.M605934200.

Gentric G, Mieulet V, Mechta-Grigoriou F (2017). Heterogeneity in cancer metabolism: new concepts in an old field. *Antioxidants & Redox Signaling* **26**: 462–485. DOI 10.1089/ars.2016.6750.

Jackson J, Lozano G (2013). The mutant p53 mouse as a pre-clinical model. *Oncogene* **32**: 4325–4330. DOI 10.1038/onc.2012.610.

Jones RG, Plas DR, Kubek S, Buzzai M, Mu J, Xu Y, Birnbaum MJ, Thompson CB (2005). AMP-activated protein kinase induces a p53-dependent metabolic checkpoint. *Molecular Cell* **18**: 283–293. DOI 10.1016/j.molcel.2005.03.027.

Jung EJ, Kwon SW, Jung BH, Oh SH, Lee BH (2011). Role of the AMPK/SREBP-1 pathway in the development of orotic acid-induced fatty liver. *Journal of Lipid Research* **52**: 1617–1625.

Kapetanovic IM, Muzzio M, Huang Z, Thompson TN, McCormick DL (2011). Pharmacokinetics, oral bioavailability, and metabolic profile of resveratrol and its dimethylether analog, pterostilbene, in rats. *Cancer Chemotherapy and Pharmacology* **68**: 593–601. DOI 10.1007/s00280-010-1525-4.

Kuhajda F (2008). AMP-activated protein kinase and human cancer: cancer metabolism revisited. *International Journal of Obesity* **32**: S36–S41. DOI 10.1038/ijo.2008.121.

Li JN, Gorospe M, Chrest FJ, Kumaravel TS, Evans MK, Han WF, Pizer ES (2001). Pharmacological inhibition of fatty acid synthase activity produces both cytostatic and cytotoxic effects modulated by p53. *Cancer Research* **61**: 1493–1499.

Lien EC, Lyssiotis CA, Cantley LC (2016). Metabolic reprogramming by the PI3K-Akt-mTOR pathway in cancer, *Metabolism in Cancer*. Cham: Springer, pp. 39–72.

Lin HS, Yue BD, Ho PC (2009). Determination of pterostilbene in rat plasma by a simple HPLC-UV method and its application in pre-clinical pharmacokinetic study. *Biomedical Chromatography* **23**: 1308–1315. DOI 10.1002/bmc.1254.

Lin VCH, Tsai YC, Lin JN, Fan LL, Pan MH, Ho CT, Wu JY, Way TD (2012). Activation of AMPK by pterostilbene suppresses lipogenesis and cell-cycle progression in p53 positive and negative human prostate cancer cells. *Journal of Agricultural and Food Chemistry* **60**: 6399–6407. DOI 10.1021/jf301499e.

Liu Y, Tong L, Luo Y, Li X, Chen G, Wang Y (2018). Resveratrol inhibits the proliferation and induces the apoptosis in ovarian cancer cells via inhibiting glycolysis and targeting AMPK/mTOR signaling pathway. *Journal of Cellular Biochemistry* **119**: 6162–6172. DOI 10.1002/jcb.26822.

LoPiccolo J, Blumenthal GM, Bernstein WB, Dennis PA (2008). Targeting the PI3K/Akt/mTOR pathway: Effective combinations and clinical considerations. *Drug Resistance Updates* **11**: 32–50. DOI 10.1016/j.drup.2007.11.003.

Luo Z, Zang M, Guo W (2010). AMPK as a metabolic tumor suppressor: control of metabolism and cell growth. *Future Oncology* **6**: 457–470. DOI 10.2217/fon.09.174.

Majumder PK, Febbo PG, Bikoff R, Berger R, Xue Q, McMahon LM, Manola J, Brugarolas J, McDonnell TJ, Golub TR (2004). mTOR inhibition reverses Akt-dependent prostate intraepithelial neoplasia through regulation of apoptotic and HIF-1-dependent pathways. *Nature Medicine* **10**: 594–601. DOI 10.1038/nm1052.

McCormack D, McFadden D (2012). Pterostilbene and cancer: current review. *Journal of Surgical Research* **173**: e53–e61. DOI 10.1016/j.jss.2011.09.054.

McCormack D, Schneider J, McDonald D, McFadden D (2011). The antiproliferative effects of pterostilbene on breast cancer *in vitro* are via inhibition of constitutive and leptin-induced Janus kinase/signal transducer and activator of transcription activation. *American Journal of Surgery* **202**: 541–544. DOI 10.1016/j.amjsurg.2011.06.020.

Mei H, Xiang Y, Mei H, Fang B, Wang Q, Cao D, Hu Y, Guo T (2018). Pterostilbene inhibits nutrient metabolism and

induces apoptosis through AMPK activation in multiple myeloma cells. *International Journal of Molecular Medicine* **42**: 2676–2688.

Memmott RM, Dennis PA (2009). Akt-dependent and -independent mechanisms of mTOR regulation in cancer. *Cellular Signalling* **21**: 656–664. DOI 10.1016/j.cellsig.2009.01.004.

Mirandola L, Yu Y, Cannon MJ, Jenkins MR, Rahman RL, Nguyen DD, Grizzi F, Cobos E, Figueroa JA, Chiriva-Internati M (2014). Galectin-3 inhibition suppresses drug resistance, motility, invasion and angiogenic potential in ovarian cancer. *Gynecologic Oncology* **135**: 573–579. DOI 10.1016/j.ygyno.2014.09.021.

Mossmann D, Park S, Hall MN (2018). mTOR signalling and cellular metabolism are mutual determinants in cancer. *Nature Reviews Cancer* **18**: 744–757. DOI 10.1038/s41568-018-0074-8.

Okawa Y, Hideshima T, Ikeda H, Raje N, Vallet S, Kiziltepe T, Yasui H, Enatsu S, Pozzi S, Breitkreutz I, Cirstea D, Santo L, Richardson P, Anderson KC (2008). Retraction: Fatty acid synthase is a novel therapeutic target in multiple myeloma. *British Journal of Haematology* **141**: 659–671. DOI 10.1111/j.1365-2141.2008.07114.x.

Pan MH, Chiou YS, Chen WJ, Wang JM, Badmaev V, Ho CT (2009). Pterostilbene inhibited tumor invasion via suppressing multiple signal transduction pathways in human hepatocellular carcinoma cells. *Carcinogenesis* **30**: 1234–1242. DOI 10.1093/carcin/bgp121.

Pei HI, Mu DM, Zhang B (2017). Anticancer activity of pterostilbene in human ovarian cancer cell lines. *Medical Science Monitor: International Medical Journal of Experimental and Clinical Research* **23**: 3192.

Peterson TR, Sengupta SS, Harris TE, Carmack AE, Kang SA, Balderas E, Guertin DA, Madden KL, Carpenter AE, Finck BN, Sabatini DM (2011). mTOR complex 1 regulates lipin 1 localization to control the SREBP pathway. *Cell* **146**: 408–420. DOI 10.1016/j.cell.2011.06.034.

Porstmann T, Santos CR, Griffiths B, Cully M, Wu M, Leevers S, Griffiths JR, Chung YL, Schulze A (2008). SREBP activity is regulated by mTORC1 and contributes to Akt-dependent cell growth. *Cell Metabolism* **8**: 224–236. DOI 10.1016/j.cmet.2008.07.007.

Priego S, Feddi F, Ferrer P, Mena S, Benlloch M, Ortega A, Carretero J, Obrador E, Asensi M, Estrela JM (2008). Natural polyphenols facilitate elimination of HT-29 colorectal cancer xenografts by chemoradiotherapy: A Bcl-2-and superoxide dismutase 2-dependent mechanism. *Molecular Cancer Therapeutics* **7**: 3330–3342. DOI 10.1158/1535-7163.MCT-08-0363.

Rattan R, Giri S, Singh AK, Singh I (2005). 5-Aminoimidazole-4-carboxamide-1-β-D-ribofuranoside inhibits cancer cell proliferation *in vitro* and *in vivo* via AMP-activated protein kinase. *Journal of Biological Chemistry* **280**: 39582–39593. DOI 10.1074/jbc.M507443200.

Redza-Dutordoir M, Averill-Bates DA (2016). Activation of apoptosis signalling pathways by reactive oxygen species. *Biochimica et Biophysica Acta (BBA)—Molecular Cell Research* **1863**: 2977–2992. DOI 10.1016/j.bbamcr.2016.09.012.

Rena G, Hardie DG, Pearson ER (2017). The mechanisms of action of metformin. *Diabetologia* **60**: 1577–1585. DOI 10.1007/s00125-017-4342-z.

Rooth C (2013). Ovarian cancer: risk factors, treatment and management. *British Journal of Nursing* **22**: S23–S30. DOI 10.12968/bjon.2013.22.Sup17.S23.

Santos CR, Schulze A (2012). Lipid metabolism in cancer. *FEBS Journal* **279**: 2610–2623. DOI 10.1111/j.1742-4658.2012.08644.x.

Shi D, Zhao D, Niu P, Zhu Y, Zhou J, Chen H (2018). Glycolysis inhibition via mTOR suppression is a key step in cardamonin-induced autophagy in SKOV3 cells. *BMC Complementary and Alternative Medicine* **18**: 248. DOI 10.1186/s12906-018-2380-9.

Sohretoglu D, Zhang C, Luo J, Huang S (2019). ReishiMax inhibits mTORC1/2 by activating AMPK and inhibiting IGFR/PI3K/Rheb in tumor cells. *Signal Transduction and Targeted Therapy* **4**: 1387. DOI 10.1038/s41392-019-0056-7.

Su CC, Hsieh KL, Liu PL, Yeh HC, Huang SP, Fang SH, Cheng WC, Huang KH, Chiu FY, Lin I (2019). AICAR induces apoptosis and inhibits migration and invasion in prostate cancer cells through an AMPK/mTOR-dependent pathway. *International Journal of Molecular Sciences* **20**: 1647. DOI 10.3390/ijms20071647.

Thupari JN, Pinn ML, Kuhajda FP (2001). Fatty acid synthase inhibition in human breast cancer cells leads to malonyl-CoA-induced inhibition of fatty acid oxidation and cytotoxicity. *Biochemical and Biophysical Research Communications* **285**: 217–223. DOI 10.1006/bbrc.2001.5146.

Tian T, Li X, Zhang J (2019). mTOR signaling in cancer and mTOR inhibitors in solid tumor targeting therapy. *International Journal of Molecular Sciences* **20**: 755. DOI 10.3390/ijms20030755.

Vander Heiden MG, Cantley LC, Thompson CB (2009). Understanding the Warburg effect: The metabolic requirements of cell proliferation. *Science* **324**: 1029–1033. DOI 10.1126/science.1160809.

Villanueva-Paz M, Cotán D, Garrido-Maraver J, Oropesa-Ávila M, de la Mata M, Delgado-Pavón A, de Lavera I, Alcocer-Gómez E, Álvarez-Córdoba M, Sánchez-Alcázar JA (2016). AMPK regulation of cell growth, apoptosis, autophagy, and bioenergetics, *AMP-Activated Protein Kinase.* In: Cham: Springer, pp. 45–71.

Vucicevic L, Misirkic M, Kristina J, Vilimanovich U, Sudar E, Isenovic E, Prica M, Harhaji-Trajkovic L, Kravic-Stevovic T, Vladimir B, Trajkovic V (2014). Compound C induces protective autophagy in cancer cells through AMPK inhibition-independent blockade of Akt/mTOR pathway. *Autophagy* **7**: 40–50. DOI 10.4161/auto.7.1.13883.

Wang MD, Wu H, Fu GB, Zhang HL, Zhou X, Tang L, Dong LW, Qin CJ, Huang S, Zhao LH, Zeng M, Wu MC, Yan HX, Wang HY (2016). Acetyl-coenzyme A carboxylase alpha promotion of glucose-mediated fatty acid synthesis enhances survival of hepatocellular carcinoma in mice and patients. *Hepatology* **63**: 1272–1286. DOI 10.1002/hep.28415.

Wang TT, Schoene NW, Kim YS, Mizuno CS, Rimando AM (2010). Differential effects of resveratrol and its naturally occurring methylether analogs on cell cycle and apoptosis in human androgen-responsive LNCaP cancer cells. *Molecular Nutrition & Food Research* **54**: 335–344. DOI 10.1002/mnfr.200900143.

Wang V, Li C, Lin M, Welch W, Bell D, Wong YF, Berkowitz R, Mok SC, Bandera CA (2005). Ovarian cancer is a heterogeneous disease. *Cancer Genetics and Cytogenetics* **161**: 170–173. DOI 10.1016/j.cancergencyto.2004.12.014.

Wang YJ, Chen RJ (2014). Pterostilbene protection and bladder cancer cells, *Cancer.* Amsterdam, Netherlands: Elsevier Inc., pp. 271–281.

Webb PM, Jordan SJ (2017). Epidemiology of epithelial ovarian cancer. *Best Practice & Research Clinical Obstetrics & Gynaecology* 41: 3–14. DOI 10.1016/j.bpobgyn.2016.08.006.

Wen W, Lowe G, Roberts C, Finlay J, Han E, Glackin C, Dellinger T (2018). Pterostilbene suppresses ovarian cancer growth via induction of apoptosis and blockade of cell cycle progression involving inhibition of the STAT3 pathway. *International Journal of Molecular Sciences* 19: 1983. DOI 10.3390/ijms19071983.

Yang WL, Perillo W, Liou D, Marambaud P, Wang P (2012). AMPK inhibitor compound C suppresses cell proliferation by induction of apoptosis and autophagy in human colorectal cancer cells. *Journal of Surgical Oncology* 106: 680–688. DOI 10.1002/jso.23184.

Yan Y, Zhou XE, Xu HE, Melcher K (2018). Structure and physiological regulation of AMPK. *International Journal of Molecular Sciences* 19: 3534. DOI 10.3390/ijms19113534.

Yu D, Zhang Y, Chen G, Xie Y, Xu Z, Chang S, Hu L, Li B, Bu W, Wang Y (2018). Targeting the PI3K/Akt/mTOR signaling pathway by pterostilbene attenuates mantle cell lymphoma progression. *Acta Biochimica et Biophysica Sinica* 50: 782–792. DOI 10.1093/abbs/gmy070.

Zadra G, Ribeiro CF, Chetta P, Ho Y, Cacciatore S, Gao X, Syamala S, Bango C, Photopoulos C, Huang Y, Tyekucheva S, Bastos DC, Tchaicha J, Lawney B, Uo T, D'Anello L, Csibi A, Kalekar R, Larimer B, Ellis L, Butler LM, Morrissey C, McGovern K, Palombella VJ, Kutok JL, Mahmood U, Bosari S, Adams J, Peluso S, Dehm SM, Plymate SR, Loda M (2019). Inhibition of *de novo* lipogenesis targets androgen receptor signaling in castration-resistant prostate cancer. *Proceedings of the National Academy of Sciences of the United States of America* 116: 631–640. DOI 10.1073/pnas.1808834116.

Zhou J, Huang W, Tao R, Ibaragi S, Lan F, Ido Y, Wu X, Alekseyev YO, Lenburg M, Hu G (2009). Inactivation of AMPK alters gene expression and promotes growth of prostate cancer cells. *Oncogene* 28: 1993–2002.